REVIEW: BIOPHYSICS

Electron Spin Resonance in Studies of Membranes and Proteins

P. P. Borbat,[1] A. J. Costa-Filho,[1] K. A. Earle,[1] J. K. Moscicki,[1,2] J. H. Freed[1]*

We provide a review of current electron spin resonance (ESR) techniques for studying basic molecular mechanisms in membranes and proteins by using nitroxide spin labels. In particular, nitroxide spin label studies with high-field/high-frequency ESR and two-dimensional Fourier transform ESR enable one to accurately determine distances in biomolecules, unravel the details of the complex dynamics in proteins, characterize the dynamic structure of membrane domains, and discriminate between bulk lipids and boundary lipids that coat transmembrane peptides or proteins; these studies can also provide time resolution to studies of functional dynamics of proteins. We illustrate these capabilities with recent examples.

ESR, a sister technique to nuclear magnetic resonance (NMR), has some key advantages and disadvantages in comparison to NMR. Because the electron has a much greater magnetic moment than a nucleus, ESR is much more sensitive per spin. In time domain experiments [e.g., free induction decays, spin echoes, or two-dimensional (2D) spectroscopy], ESR's time scale is nanoseconds versus NMR's time scale of milliseconds. Thus, ESR is naturally suited for studying faster dynamics. The absence of unpaired electrons in most chemical and biological materials would appear to be a major impediment for the applicability of ESR, but it can be used as an important virtue. Spin labeling of selected molecules with a small spin-bearing moiety that has a simple ESR signal, as well as the limited number of spins contributing to the ESR experiment, enables a broad range of problem-targeted studies. Most biological studies have been performed with conventional ESR (*1–5*), but we consider newer developments here.

ESR spectroscopy, based on nitroxide spin labeling, is largely driven by the sensitivity of the nitroxide label to its surroundings. This comes about in a number of ways. The interaction of the unpaired electron spin of the nitroxide with the ^{14}N magnetic nucleus ($I = 1$) leads to an electron–nuclear dipolar (or hyperfine, hf) tensor, which, for a rapidly tumbling molecule, averages to a nonzero value (the hf splitting). This is also the case for the g tensor of the electron spin (analogous to the chemical shift tensor in NMR), which, when averaged, yields the g shift. If the investigated system (e.g., a membrane) is macroscopically aligned, then one can observe the different "single-crystal–like" spectra obtained for each orientation of the system with respect to the constant magnetic field. The homogeneous line broadening (hb) of the spectra would then reflect the motional dynamics.

ESR spectra are known to change dramatically as the tumbling motion of the probe slows, thus providing great sensitivity to fluidity in the neighborhood of the spin probe (*1*). This is different from NMR, where the molecular motions in liquids lead to nearly complete averaging of the motion-dependent terms in the spin Hamiltonian. Their residual effects are then reflected only in the relaxation times, T_1 and T_2, and may be accounted for by Redfield perturbation theory. However, the equivalent terms for ESR are much larger, frequently leading to effects that are too dramatic to be addressed by perturbation theory. Instead, an approach based on the stochastic Liouville equation, known as slow-motional theory, has been developed (*6–10*), which shows that the dramatic line shape changes are particularly sensitive to the microscopic details of the dynamics.

These methods of analysis enable a quantitative assessment of ESR spectra in terms of motional rates of spinning of the nitroxide moiety, the end-over-end tumbling of the tagged molecule, and local environmental constraints to the motion. For a spin-labeled protein, for example, the motions could be the spinning about the tether attaching the nitroxide and the overall tumbling of the protein. In a bilayer, typical of a cell membrane, reorientation of the lipids is constrained by the surrounding lipids and other molecules. The motional rates lead to a rotational diffusion tensor, whereas the motional constraints lead to an orientational order parameter.

The changes in magnitude of the hf splitting and g shift can be used to monitor features of the local surroundings, such as its polarity (*11, 12*). In addition, unpaired electron spins from different nitroxides (on the same or different molecules) interact weakly through long-range magnetic dipolar interactions or strongly through short-range Heisenberg spin exchange. In fluid media, these latter interactions can be used to monitor microscopic translational dynamics (*13, 14*). In frozen or very viscous media, the dipolar interactions can be used to measure distances (*4*), either by continuous wave (cw) ESR (*4, 5, 10, 15, 16*) or pulsed ESR (*4, 17*).

Often, one must deal with the complications of samples that are MOMD [i.e., microscopically ordered but macroscopically disordered (*7, 9*)]. Membrane vesicles offer a physical example of this property. Spin-labeled moieties in the different vesicle regions may then be oriented at all angles with respect to the magnetic field, thus providing a "powder-like" spectrum with inhomogeneous line broadening (ib) superimposed on the hb. The degree of the ib is determined by the extent of local (microscopic) ordering. This ib masks the hb, resulting in reduced resolution to dynamic and ordering parameters. Despite this, modeling of the heterogeneity and of the dynamic effects to fit the ESR spectrum can yield important insights (*18, 19*).

Technical Advances

New instrumentation greatly enhances these capabilities and allows ESR to be applied more effectively to the complex structural and dynamic aspects of membranes and proteins. There are two principal avenues of contemporary ESR developments (*20, 21*). The first is the extension of cw ESR to high fields/high frequencies (*22–24*). The second is time domain, or pulsed ESR (*20, 21*).

High-frequency (HF) ESR. The primary advantages of extending ESR to HF (*22–24*) include an increased signal-to-noise ratio and improved spectral resolution. As one moves to HF, two important features emerge. First, for a given diffusion rate, as the ESR frequency increases, spin-label motion appears to become slower (*25*); that is, HF ESR spectra act as a faster "snapshot" of the dynamics (cf. Fig. 1, right). At the low-frequency end, one observes motionally narrowed spectra, whereas, at the high-frequency end, the spec-

[1]Baker Laboratory of Chemistry and Chemical Biology, Cornell University, Ithaca, NY 14853–1301, USA. [2]Smoluchowski Institute of Physics, Jagellonian University, Ulica Reymonta 4, 30–059 Krakow, Poland.

*To whom correspondence should be addressed. E-mail: jhf@ccmr.cornell.edu

tra display very slow motion, almost at the rigid limit (due to the increased importance of the g tensor).

The second feature is the great improvement in orientational resolution of the nitroxide spectrum (*22–24, 26*), illustrated in Fig. 1, left. At 250 GHz, the regions corresponding to nitroxides with their x axis $\| \boldsymbol{B}_0$ (i.e., x axis is parallel to the main magnetic field, $\mathbf{B}_0$), y axis $\| \boldsymbol{B}_0$, and z axis $\| \boldsymbol{B}_0$ are well separated, because of the dominant role of the g tensor; this separation is not observed at 9 GHz. Then, because one can discern the axis (or axes) about which the motion occurs, the 250-GHz slow-motional spectra are much more sensitive to the details of the motions than are those at microwave frequencies (*26, 27*).

Pulsed ESR. Pulsed ESR techniques (*20, 21*), especially in two dimensions, that have many analogies to 2D NMR are a second highlight. To achieve greater reliability in analyzing spectra, one must improve spectral resolution in studies of the dynamic structure of biosystems. Foremost is the need to distinguish between the mechanisms of hb and ib, which is achieved with the aid of spin echoes. A technique that accomplishes this is 2D electron-electron double resonance (ELDOR) (*28–31*), which also supplies off-diagonal peaks (cross peaks) that directly report on translational and rotational motions of labeled biomolecules.

Double quantum coherence (DQC) is a new and powerful application of pulsed ESR for distance measurements between interacting spins in frozen media (*32, 33*). The virtue of DQC ESR shown in Fig. 2 is that it permits detection of only the weak dipolar interaction between the two nitroxides in the ESR signal. Oscillations in echo amplitude versus echo time are due to this dipolar interaction (Fig. 2). A detailed analysis of DQC indicates that distances can be measured to ~80 Å, comparable to the capabilities of fluorescence energy transfer (*33*).

Illustrative Applications

HF cw ESR and complex dynamics in proteins and membranes. The snapshot feature of cw ESR encourages a multifrequency approach to the study of the complex modes of motion of proteins, DNA, and other polymers, enabling the decomposition of these modes according to their different time scales (*25*). For example, in the case of proteins, the higher frequency ESR spectra should "freeze out" the slow overall tumbling motions, leaving only the faster internal modes of motion. Alternatively, ESR performed at lower frequencies would be sensitive to the motions on a slower time scale. This is in contrast to aqueous solution NMR, where all modes are usually in the fast motional limit and contribute only to T_1 and T_2.

The virtues of such an approach were demonstrated in a study at 9 and 250 GHz on spin-labeled mutants of T4 lysozyme in aqueous solution (*34*). On the short time scale of the 250-GHz ESR experiment, the overall tumbling was too slow to affect the spectrum; thus, a MOMD analysis provided a satisfactory modeling of the overall tumbling, and HF-enhanced spectral resolution reported on the internal dynamics (Fig. 3). The analysis of the 9-GHz spectra was more complex, because the longer time scale did not freeze out the overall tumbling motion. The slowly relaxing local structure (SRLS) model (*25*) simultaneously incorporated both the internal and overall motions (Fig. 3, bottom). By fixing the internal motional parameters at the values obtained from the 250-GHz data, fits to the 9-GHz line shapes generated by SRLS successfully yielded the rate for the global dynamics. Thus, exploiting the time scale separation allowed more information to be extracted [see (*35–38*)].

In a demonstration of the excellent orientational resolution at 250 GHz, macroscopically aligned membranes containing a mixture of head groups [zwitterionic phosphatidylcholine (PC) and negatively charged phosphatidylserine (PS)] were studied by using the cholesterol-like spin label, cholestane (CSL) (*26*). The direction of alignment of the CSL molecules could be clearly discerned as the orientation of the membrane normal was changed with respect to the magnetic field. The CSL in PC-rich membranes exhibited typical behavior; that is, its long axis was parallel to the bilayer normal, and its rotational diffusion rates R were slow ($R \sim 10^6$ to $10^7\ s^{-1}$). However, the behavior in PS-rich membranes is unusual and was interpreted in terms of a strong local biaxial environment. Although predicted from molecular dynamics simulations, this gives experimental evidence for local biaxiality. By contrast, given the poorer orientational resolution at 9.1 GHz, it was not possible to distinguish such detail from the 9.1-GHz experiment.

Two-dimensional Fourier transform (FT) ESR and dynamic structure of membranes. Two-dimensional time domain ESR methods allow one to study both dynamics and ordering in membrane vesicles (*30, 31*). In general, 2D ELDOR spectra from membrane vesicles exhibit more dramatic variations due to changes in membrane properties than do spectra obtained by cw ESR. A simple interpretation of these spectra is thus possible merely by pattern recognition. For example, 2D ELDOR contour plots are shown for the spin-labeled lipid, 16 PC, in pure lipid vesicles (Fig. 4A) and for a lipid-cholesterol (1:1) mixture (Fig. 4B). The former is in the standard liquid crystalline (LC) phase, whereas the latter is in a "liquid ordered" (LO) phase. This type of LO phase has been found to play an important role in cellular signaling and in membrane trafficking (*19, 39*). Visually, the spectra are qualitatively different, emphasizing that the LO phase exhibits substantially greater ordering, but comparable rotational mobility, in comparison with the LC phase. Quantitative spectral fits confirm that the

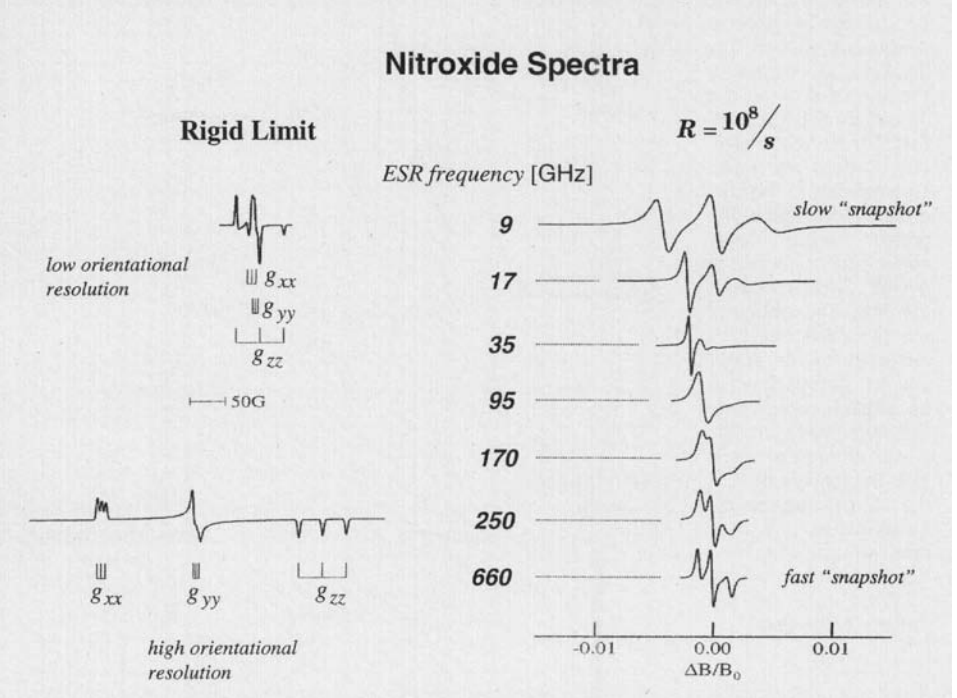

Fig. 1. Nitroxide cw ESR spectra change dramatically with frequency. (**Left**) Simulations illustrate the increased orientational sensitivity of ESR on going from low (9 GHz) to high (250 GHz) frequencies. The derivative spectra are characteristic of a spin label in a frozen amorphous matrix (i.e., the rigid limit). The triplet hyperfine splittings (marked by a set of three vertical lines) are due to the interaction of the unpaired electron with the ^{14}N nucleus. (**Right**) The derivative ESR simulations for characteristic ESR frequencies demonstrate the snapshot property of ESR when studying tumbling spin-labeled molecules. The large variations that the spectrum undergoes as the frequency is changed are very sensitive to the character of the motion.

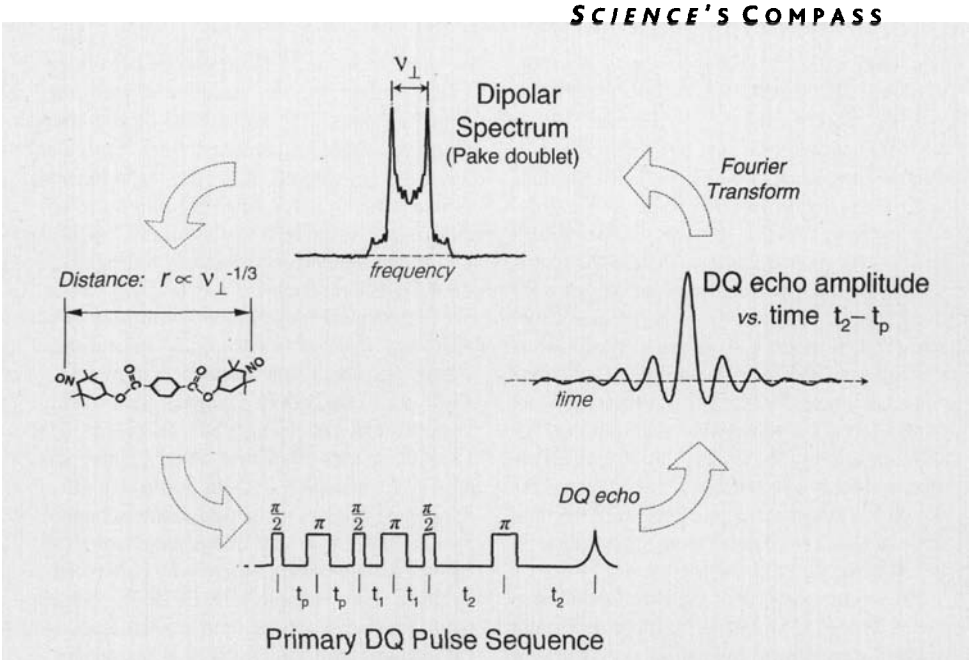

Fig. 2. Principles of the pulsed DQC ESR experiment. **(Left)** The doubly labeled molecule is dissolved in a frozen amorphous matrix. **(Bottom)** The six-pulse DQC sequence preserves contributions to the double quantum echo signal arising solely from the dipolar interaction between the pair of nitroxide spin labels. One varies the time intervals t_p and t_2 such that the total time of the pulse sequence remains constant. **(Right)** The maximum of the echo signal is recorded as a function of $t_2 - t_p$. **(Top)** A Fourier transform of this echo signal yields the Pake-type dipolar spectrum in the frequency domain. The separation $\nu_\perp$ of the two sharp peaks is directly related to the distance r between the labels, $r \propto \nu_\perp^{-1/3}$. (The echo signal and the dipolar spectrum shown here were measured for the molecule on the left, for which $r \cong 16.2 \pm 0.5$ Å.)

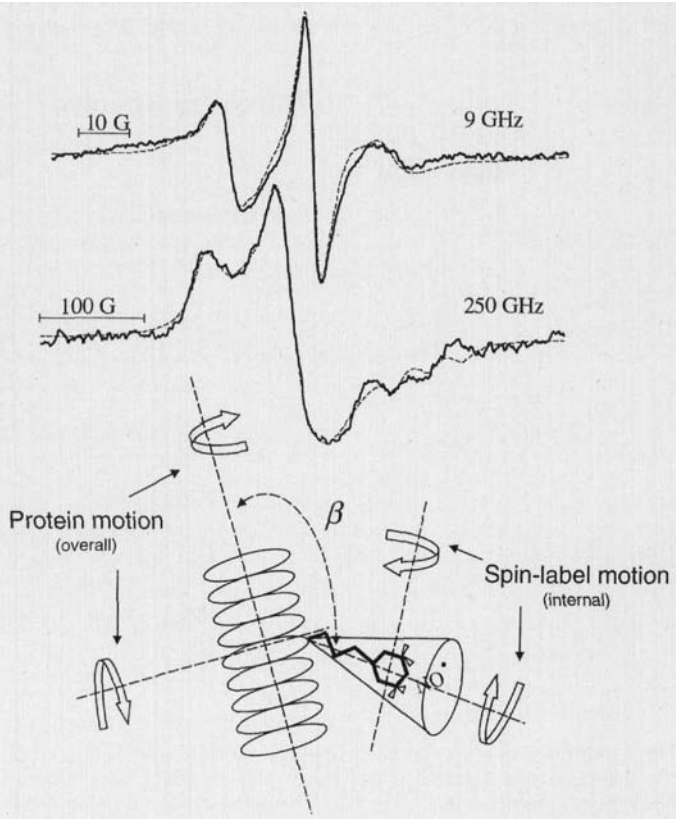

Fig. 3. A multifrequency ESR study of nitroxide spin-labeled T4 lysozyme in aqueous solution. The derivative spectra are for the spin label on residue 44 and are taken at 10°C (*34*). The relevant molecular motions are shown schematically in the lower part of the figure. The protein tumbles slowly about its principal axes of overall diffusion; this is the SRLS. The motion of the spin label moiety is restricted by its tether and its surroundings to be within a cone, whose main axis makes an angle β with the protein main axis. The spatial extent of the internal rotational diffusion modes and their rates are distinguished from the protein overall tumbling rates as described in the text.

increased microscopic ordering leads to increased ib affecting the spectra from the LO phase. Furthermore, the restriction of the range of orientational motion, due to the microscopic ordering in the LO phase, shows up as a much slower development of cross peaks.

Two-dimensional FT ESR and lipid-protein interactions. The merits of 2D FT ESR spectroscopy are well demonstrated in studies of the effect of the peptide gramicidin A (GA) on the dynamic structure of model membranes. Besides bulk lipids, boundary lipids that coat the peptide are present but difficult to resolve in cw ESR. Two-dimensional ELDOR at 9.3 GHz (*31*) yielded dramatic changes in spectra as GA was added to vesicles, because of changes in the dynamic structure of bulk lipids. However, newer 2D ELDOR results at 17.3 GHz, with improved time resolution, show the presence of two components (*40*). The boundary lipid appears as a broader spectral component, characteristic of a more slowly reorienting lipid with greater motional restriction (Fig. 4, C and D). Aligning the membranes enables resolution of boundary lipids, even in the presence of small amounts of GA (1 to 4 mole percent) (*30, 40*).

Multiple-quantum ESR and distance measurements. The determination of intra- and intermolecular distances has become an important application of contemporary ESR spectroscopy. Areas of interest include the structure of protein complexes and the functional dynamics of proteins that are neither soluble nor crystallized (*4, 5, 10, 15, 16*).

Strong DQC signals for a variety of bilabeled nitroxide molecules in both disordered and oriented solids have been achieved recently (*32, 33*) (cf. Fig. 2). For a benchmark rigid linear biradical, piperidinyl-CO_2-(phenyl)$_4$-O_2C-piperidinyl, a distance of 28.8 ± 0.5 Å between the two nitroxide groups was obtained (versus 28.06 Å from molecular modeling). For a semiflexible bilabeled synthetic peptide [MTSL-CPPPPC-MTSL in frozen solution at −82°C (MTSL, the [1-oxyl-2,2,5,5-tetramethyl-pyrrole-3-methyl] methanethiosulfonate spin label; C, Cys; and P, Pro) relevant to biophysical studies, a mean separation of 22.6 Å between the two nitroxide groups and a distribution half-width of 2 Å (which smears out the Pake doublet) were found. Current sensitivities require ~300 pmol of bilabeled molecules, but it is estimated that, in the future, studies with samples that are approximately an order of magnitude less will be feasible (*33*).

Future Prospects

Given the virtues of time domain ESR (such as direct determination of relaxation rates and differentiation between hb and ib) compared to the virtues of HF cw ESR (enhanced orientational selectivity and greater sensitivity to nuances of the molecular dynamics), it would be desirable to extend pulse techniques to higher frequencies (*41*). However, as the frequency is increased, spin-labeled biomolecules in fluid media would have shorter transverse decay times, because of enhanced hb and ib. Thus, even shorter time resolution and greater spectral bandwidths would be required, hence shorter and more intense radiation pulses (*30*). Progress in devel-

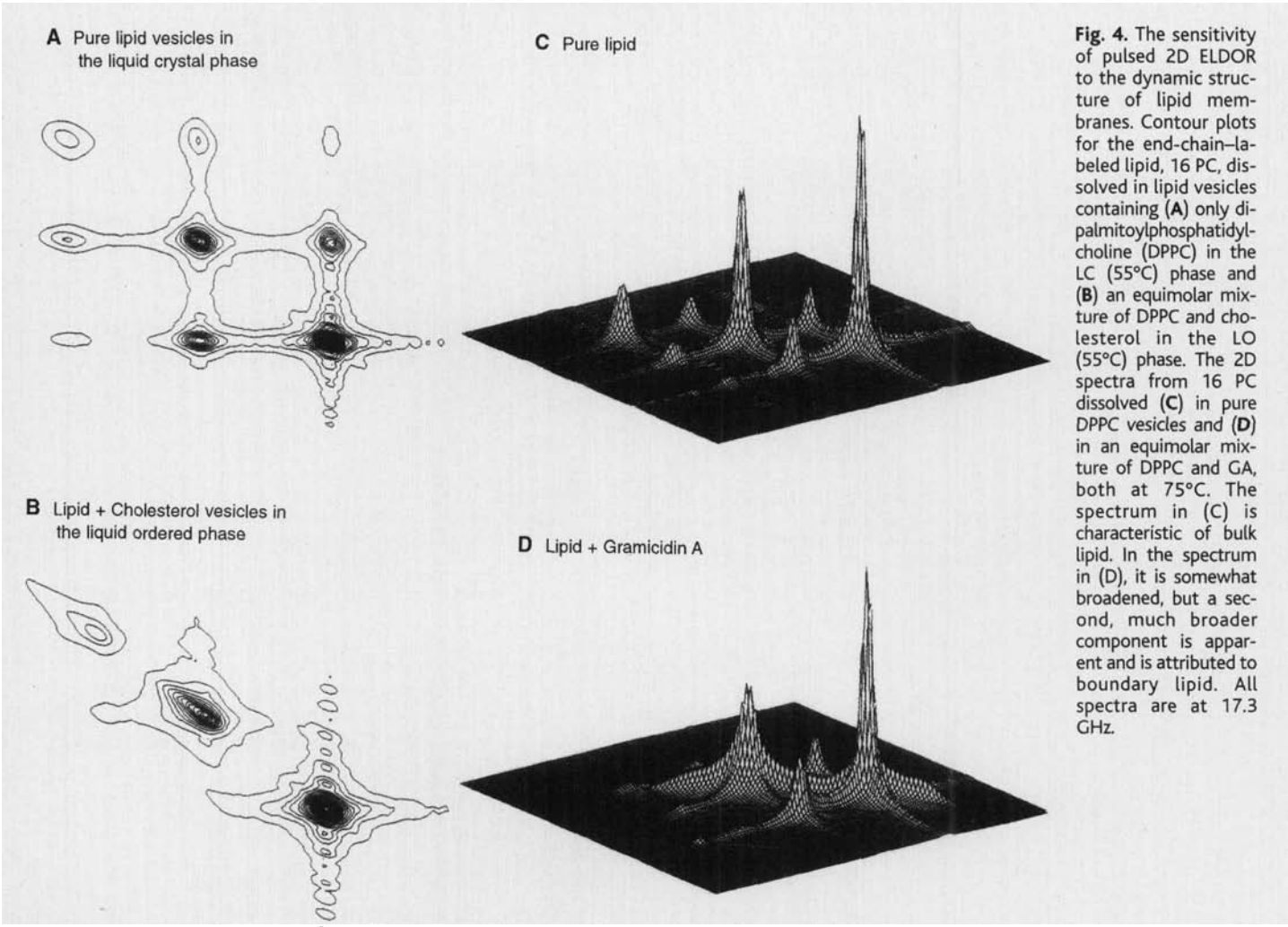

Fig. 4. The sensitivity of pulsed 2D ELDOR to the dynamic structure of lipid membranes. Contour plots for the end-chain–labeled lipid, 16 PC, dissolved in lipid vesicles containing (**A**) only dipalmitoylphosphatidylcholine (DPPC) in the LC (55°C) phase and (**B**) an equimolar mixture of DPPC and cholesterol in the LO (55°C) phase. The 2D spectra from 16 PC dissolved (**C**) in pure DPPC vesicles and (**D**) in an equimolar mixture of DPPC and GA, both at 75°C. The spectrum in (C) is characteristic of bulk lipid. In the spectrum in (D), it is somewhat broadened, but a second, much broader component is apparent and is attributed to boundary lipid. All spectra are at 17.3 GHz.

oping a coherent pulsed high-power spectrometer at 95 GHz has recently been reported (*42*).

The fast time scales of 2D FT ESR (*30*) are poised to address the functional dynamics (*5*) of proteins. Nanosecond resolution is achievable in following the time evolution of a (small) region of the spectrum, and 0.1- to 1-μs resolution is possible for the entire nitroxide spectrum. cw ESR studies of the transient behavior of bilabeled bacteriorhodopsin following light activation were able to resolve key distance changes occurring on the 1-ms to 1-s time scale (*43*, *44*). FT ESR combined with DQC should enable studies in the submicrosecond range. Similar applications for short time dynamics would be for rapid mixing and stopped-flow experiments (*45*), limited only by the time resolution of these methods.

References

1. L. J. Berliner, Ed., *Spin Labeling: Theory and Applications* (Academic Press, New York, 1976).
2. ———, J. Reuben, Eds., *Spin Labeling: Theory and Applications*, vol. 8 of *Biological Magnetic Resonance* (Plenum, New York, 1989).
3. L. J. Berliner, Ed., *Spin Labeling: The Next Millennium*, vol. 14 of *Biological Magnetic Resonance* (Plenum, New York, 1998).
4. G. R. Eaton, S. S. Eaton, L. J. Berliner, Eds., *Distance Measurements in Biological Systems by EPR*, vol. 19 of *Biological Magnetic Resonance* (Kluwer, New York, 2000).
5. W. L. Hubbell, D. S. Cafiso, C. Altenbach, *Nature Struct. Biol.* **7**, 735 (2000).
6. J. H. Freed, in (*1*), pp. 53–132.
7. D. J. Schneider, J. H. Freed, in (*2*), pp. 1–76.
8. A. H. Beth, B. H. Robinson, in (*2*), pp. 179–253.
9. D. E. Budil, S. Lee, S. Saxena, J. H. Freed, *J. Magn. Reson.* **A120**, 155 (1996).
10. E. Hustedt *et al.*, *Biophys. J.* **74**, 1861 (1997).
11. O. H. Griffith, P. J. Dehlinger, S. P. Van, *J. Membr. Biol.* **15**, 159 (1974).
12. K. A. Earle *et al.*, *Biophys. J.* **66**, 1213 (1994)
13. J. H. Freed, *Annu. Rev. Biophys. Biomol. Struct.* **23**, 1 (1994).
14. D. Marsh, in (*2*), pp. 255–303.
15. M. D. Rabenstein, Y.-K. Shin, *Proc. Natl. Acad. Sci. U.S.A.* **92**, 823 (1995).
16. H. J. Steinhoff *et al.*, *Biophys. J.* **73**, 3287 (1997).
17. A. D. Milov, A. G. Maryasov, Yu. D. Tsvetkov, *Appl. Magn. Reson.* **15**, 107 (1998).
18. M. Ge, J. H. Freed, *Biophys. J.* **76**, 264 (1999).
19. M. Ge *et al.*, *Biophys. J.* **77**, 925 (1999).
20. A. J. Hoff, Ed., *Advanced EPR, Applications in Biology and Biochemistry* (Elsevier, New York, 1989).
21. L. Kevan, M. K. Bowman, Eds., *Modern Pulsed and Continuous-Wave Electron Spin Resonance* (Wiley, New York, 1990).
22. D. E. Budil *et al.*, in (*20*), pp. 307–340.
23. Y. S. Lebedev, in (*21*), pp. 365–404.
24. International Experts' Workshop: Present and Future of HFEPR Instrumentation, S. S. Eaton, G. R. Eaton, Eds., *Appl. Magn. Reson.* **16**, 159 (1999).
25. Z. Liang, J. H. Freed, *J. Phys. Chem. B* **103**, 6384 (1999).
26. J. B. Barnes, J. H. Freed, *Biophys. J.* **75**, 2532 (1998).
27. K. A. Earle *et al.*, *J. Chem. Phys.* **106**, 9996 (1997).
28. J. Gorcester, G. L. Millhauser, J. H. Freed, in (*20*), pp. 177–242; in (*21*), pp. 119–194.
29. M. K. Bowman, in (*21*), pp. 1–42.
30. P. P. Borbat, R. H. Crepeau, J. H. Freed, *J. Magn. Reson.* **127**, 155 (1997).
31. B. Patyal, R. H. Crepeau, J. H. Freed, *Biophys. J.* **73**, 2201 (1997).
32. P. P. Borbat, J. H. Freed, *Chem. Phys. Lett.* **313**, 145 (1999).
33. P. P. Borbat, J. H. Freed, in (*4*), pp. 383–459.
34. J. Barnes *et al.*, *Biophys. J.* **76**, 3298 (1999).
35. J. Pilar *et al.*, *Macromolecules* **33**, 4438 (2000).
36. Z. Liang, A. M. Bobst, R. S. Keyes, J. H. Freed, *J. Phys. Chem. B* **104**, 5372 (2000).
37. D. E. Budil *et al.*, *Biophys. J.* **78**, 430 (2000).
38. M. Beunati *et al.*, *J. Magn. Reson.* **139**, 281 (1999).
39. D. A. Brown, E. London, *Annu. Rev. Cell Dev. Biol.* **14**, 111 (1998).
40. P. P. Borbat, R. H. Crepeau, M. Ge, J. H. Freed, paper presented at the 22nd International EPR Symposium, Denver, CO, 1 to 5 August 1999.
41. T. F. Prisner, *Adv. Magn. Opt. Reson.* **20**, 245 (1997).
42. K. A. Earle, C. Dunnam. P. P. Borbat, J. H. Freed, *Am. Phys. Soc. Abstr.* **45**, 542 (2000).
43. T. E. Thorgeirsson *et al.*, *J. Mol. Biol.* **273**, 951 (1997).
44. R. Mollaaghababa *et al.*, *Biochemistry* **39**, 1120 (2000).
45. V. M. Grigoryants, A. V. Veselov, C. P. Scholes, *Biophys. J.* **78**, 2702 (2000).